Observation of Precursor of the Kamchatka Earthquake by Monitoring an Optical Fiber Link in the Mediterranean Sea

Antonio Mecozzi[(1,*)], Cristian Antonelli[(1)], Alberto Marullo[(2)], Danilo Decaroli[(2)], Luca Palmieri[(3)], Luca Schenato[(3)], Siddharth Varughese[(4)], Pierre Mertz[(4)], Mohammad M. Hosseini[(5)], Antonio Napoli[(5)]

[(1)] Department of Physical and Chemical Sciences, University of L'Aquila, v. Vetoio, L'Aquila, 67100, Italy;
[(2)] Sparkle, v. di Macchia Palocco 223, Roma, 00125, Italy
[(3)] Department of Information Engineering, University of Padova, v. Gradenigo 6/b, Padova, 35131, Italy
[(4)] Nokia, MD, USA; [(5)] Nokia, Munich, Germany; [(*)] antonio.mecozzi@univaq.it

Abstract *By monitoring the state of polarization of cables belonging to the MedNautilus submarine system in the Mediterranean Sea, we unambiguously observed the signature of the recent M_w 8.8 Kamchatka earthquake in two different cables. A clear precursor of the earthquake is observed in one of the cables.*

Introduction

Sensing using fiber-optic communication links, especially undersea, is a rapidly growing research topic of interest[1]–[9]. A special class of sensing techniques uses information that has already been generated within the digital signal processing (DSP) ASIC of commercial transponders[10]. This is because the long-haul optical communication systems that are deployed nowadays use coherent detection and DSP algorithms to, for example, reconstruct and compensate for the phase and polarization changes that light undergoes during its journey[11]. These polarization changes are described by the Jones matrix, which is therefore sensitive to all perturbations that act on the optical fiber along its path. This matrix can be extracted, with minimal modifications to the transponder hardware, from coherent optical communication systems during their normal operation, without altering the data flow in any way. In addition, since no information on the transmitted data can be inferred from the Jones matrix, its extraction at the receiver does not compromise traffic privacy. The analysis of a subset of information that can be extracted from the Jones matrix, duly processed, has shown impressive sensing capabilities. In particular, the analysis of the output polarization – that corresponds to a linear polarization at the input – has shown its potential for detecting various environmental perturbations. In ref.[2], several earthquakes were detected near the Curie undersea optical cable, which connects Los Angeles, California, to Valparaiso, Chile. Furthermore, minuscule modulations were revealed at ultra-low frequencies of hydrostatic pressure acting on the cable, resulting from ocean swells and from semidiurnal modulations originating from ocean tides in the region close to the Los Angeles terminal of the cable[3],[12].

In this work, we use the innovative processing introduced in[13] to analyze Jones matrices extracted with a sampling period of 500 ms from two optical coherent transponders located in Catania, Italy. These are part of the two segments of Sparkle's MedNautilus submarine telecommunication system connecting Haifa and Tel Aviv, Israel, to Catania. The transponders used in this trial are described in[10], and the optical cable is, in the wet part, except for a few hundred meters close to the coast, a lightweight jelly-filled optical cable. The unprecedented sensitivity obtained, together with the technique's ability to detect pressure modulations that are spatially coherent over hundreds of kilometers, allowed us to clearly observe a precursor of the recent magathrust Kamchatka earthquake, which occurred at a distance of ∼9000 km. Fig. 1 illustrates the geographical layout.

Fig. 1: Representation of the scenario: (red) distance Kamchatka → Haifa; (black) optical link Catania → Haifa.

Method

Our analysis relies on extracting the 3D rotation vector from the Jones matrix, which characterizes the change in polarization between the transmitter and the receiver[13],[14]. The evolution of polarization from input to output can be described as a rotation in Stokes space, a 3D representation, with the corresponding rotation vector derived from the Jones matrix[14]. To account for the effects of time-dependent environmental changes only, we compensated for the quasi-static input-output polarization changes using a Jones matrix obtained

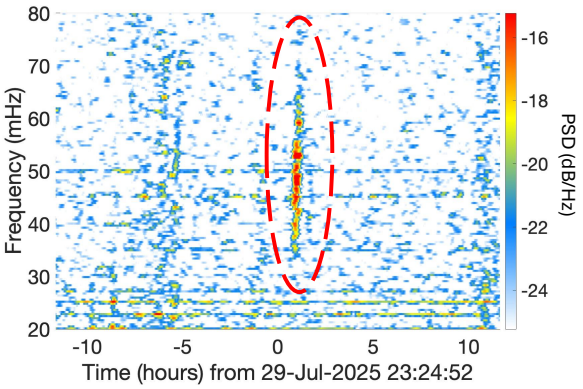

Fig. 2: Spectrogram of the rotation vector of the Jones matrix obtained from the Catania → Haifa terminal, ∼ 9,000 km from the epicenter. The time axis spans 24h centered on the earthquake (at 0h). The red oval highlights the Rayleigh wave originated by the earthquake and detected 9,000 km away.

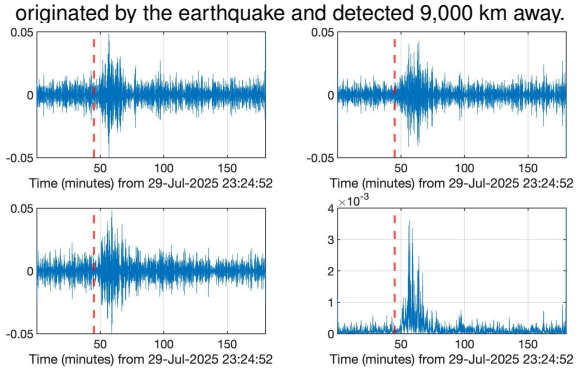

Fig. 3: Traces of the three components of the rotation vector and the square modulus of the rotation vector (bottom right), obtained from Catania → Haifa terminal, filtered in the band between 30 to 70 mHz, displayed up to 3 hours after the earthquake. The 0 of the time axis is again at the earthquake time. The red dashed vertical lines denote 45 minutes after the earthquake.

by averaging the rotation vector over a 2-hour time interval. Finally, we extracted the rotation vector from the compensated Jones matrix that describes the perturbations and computed its spectrogram, defined as the short-time Fourier transform of the temporal autocorrelation function of the rotation vector, by adding the spectrograms of its three components. In contrast to the technique used in previous studies on the Curie cable, this method fully characterizes the polarization evolution along the fiber, not just the output linear polarization at the input. As a result, while the contrast of the spectrograms was only 10 dB with the technique of Refs.[2],[3],[12], here we achieved a contrast of 30 dB. In addition, this technique allowed us to use a much longer averaging time of the rotation vector that we used for compensation, 2 hours against 300 seconds in Refs.[2],[3],[12]. This improved the low-frequency sensitivity from a few tens of mHz to fractions of mHz.

Results

On 29 July 2025, at 23:24:52 UTC, a M_w 8.8 megathrust earthquake struck the Kamchatka Peninsula in Russia. It was one of the largest earthquakes ever recorded. In Fig. 2, we show

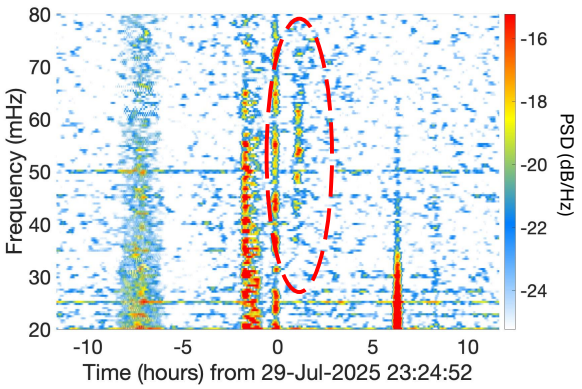

Fig. 4: Spectrogram of the rotation vector of the Jones matrix obtained from the Catania terminal of the Catania-Tel Aviv link. The time axis spans 24h centered on the earthquake (at 0h). The red oval highlights the Rayleigh wave.

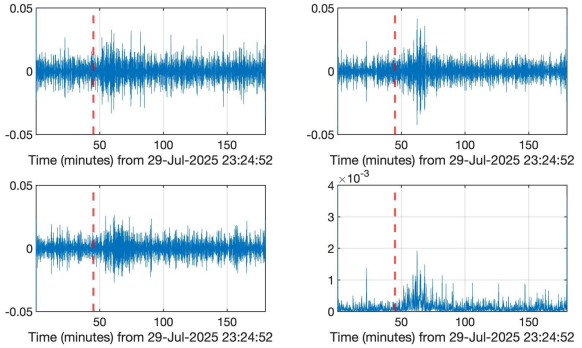

Fig. 5: Traces of the three components of the rotation vector and the square modulus of the rotation vector (bottom right), obtained from the Catania → Tel Aviv terminal, filtered in the band between 30 to 70 mHz, displayed up to 3 hours after the earthquake. The 0 of the time axis is the earthquake time. The red dashed lines indicate 45 minutes after the earthquake.

the spectrogram of the rotation vector obtained from the Catania terminal of the Catania-Haifa link, ∼9,000 km away from the epicenter. The time axis spans one full day centered on the earthquake, with zero corresponding to the earthquake time. Between 30 and 70 mHz, a clear signature of a wave train is visible (red oval), with a slight anomalous dispersion feature.

Figure 3 shows the traces (in radians) of the three components of the rotation vector filtered in the band between 30 and 70 mHz and, in the subplot at the bottom right, the square modulus of the filtered rotation vector, during a time span of six hours centered at the time of the earthquake, showing a clear signature of the event. The red dashed vertical lines mark the arrival of the perturbation, which occurred about 45 minutes after the earthquake. This time of arrival is consistent with the arrival of a train of Rayleigh waves. These are surface seismic waves that propagate along the boundary of a solid (or between two solids), in a way analogous to gravity waves on the surface of a fluid[15]. These waves have a transverse component, hence they couple with the seawater pressure, and the cable detects the consequent pressure changes. Assuming a distance of the earthquake epicenter of approximately 9,000 km,

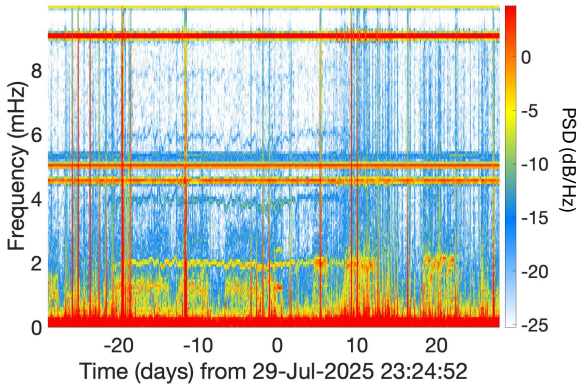

Fig. 6: Spectrogram obtained by decimating by $N = 100$ the samples of the rotation vector of the Jones matrix extracted by the Catania terminal of the Catania-Haifa link, from July 1st to midnight on August 26, 2025. The zero of the time axis is, as before, at the time of the earthquake.

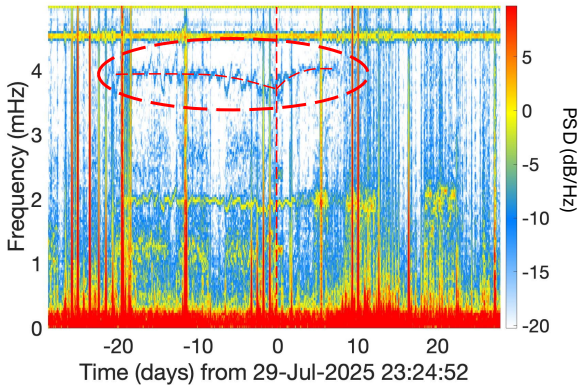

Fig. 7: Zoom of the low frequency portion of the spectrogram in Fig. 6, obtained by decimating the samples by $N = 200$.

the estimated speed of the Rayleigh wave train is approximately $v_R = 3.3$ km/s, a realistic value for a Rayleigh wave traveling in the deep crust or in the mantle. Being $\Delta f \simeq (70 - 30)$ mHz, the coherence length of the source is $D \simeq v_R/\Delta f \simeq 83$ km. Similar features are observed in the Catania receiver of the Catania-Haifa link, as shown in Figs. 4 – 5.

The spectrograms obtained from the Haifa and Tel Aviv receivers of the same links show, as expected, the same features, and the temporal traces are essentially equal. The corresponding plots are again not included here due to space limitations.

Even more interesting is the analysis of the spectrograms of the rotation vector extracted from the receivers of the Catania-Haifa link in the month before and after the earthquake. Here, we focus on the Catania receiver. Figure 6 shows the spectrogram of the rotation vector of the Catania-Haifa link from July 1 to August 26, 2025. The zero of the time axis is again at the time of the earthquake. Besides straight lines at frequencies multiple of 4.5 and 5 mHz, which are artifacts of the phase recovery algorithm, the striking feature is the appearance, about 20 days before the earthquake, of multiple resonances at about 2, 4, 6, and 8 mHz, which disappear a few days after the earthquake.

Figure 7 is a zoom in on the low-frequency portion of Fig. 6. Apart from a nearly diurnal modulation of the frequency, the spectrogram shows that the frequency of the resonances reveals a minimum at approximately the time of the earthquake. This fact, especially evident in the resonance at about 4 mHz overlayed with a dashed line and highlighted with an oval in Fig. 7, is a strong indication that the resonances were generated by the processes that were preparing for the earthquake, which were observed 9,000 km away.

We interpret the above results as follows. During preparation for the earthquake, the fault starts to radiate Rayleigh waves with a wide spectrum. The Rayleigh waves that propagate to the Mediterranean Sea are locally trapped in a basin which acts as a resonator, amplifying the Rayleigh wave at frequencies $f_n = nv_R/(2L)$, where L is the length of the basin calculated from the boundaries orthogonal to the direction of the incoming Rayleigh wave, and v_R is the speed of the Rayleigh wave. The fact that we observe up to the fourth order of the resonance is consistent with the high Q that this process (whose sea-wave counterpart is the seiche phenomenon responsible for the *acqua alta* in the Venetian lagoon) may have. The temporal variation of the resonance frequencies may indicate that the direction of the incoming Rayleigh waves changes over time. This change may be caused by the motion of the source radiating the Rayleigh wave in preparation for the earthquake and that the motion reverses after the earthquake. The diurnal modulation of the resonance may suggest a role of solid tides in the preparation of the earthquake, producing a modulation of the position of the Rayleigh wave emitter position.

Estimating the length of the basin responsible for the resonance is a challenging task. Standing Rayleigh waves are trapped locally on the seabed, whose characteristics determine the wave phase speed. In its section near the Haifa terminal, the cable runs through a region close to the Nile Delta, where the Nile River provides a significant source of sediments. Since the Catania-Haifa cable was installed about 25 years ago, it is likely to be covered by sediments. The resulting acoustic impedance match, which produces a high acoustic coupling with the seafloor, explains the high sensitivity of the cable to pressure modulation. Assuming $v_R = 3.3$ km/s, we obtain $f_1 = v_R/(2L) = 1$ mHz for $L = 700$ km, which is the width of the Mediterranean Sea between Egypt and Turkey in the direction to the earthquake epicenter.

Conclusion

In conclusion, the application of an ultrasensitive technique to the Jones matrices obtained by monitoring the state of polarization of a submarine optical cable allowed us not only to detect but also to observe a precursor of the Kamchatka earthquake from about 9,000 km distance.

Acknowledgements

This work has been carried out within the framework of the ECSTATIC project, which received funding from the Horizon Europe Framework Program of the European Union under grant agreement No. 101189595.

References

[1] G. Marra, C. Clivati, R. Luckett, A. Tampellini, J. Kronjäger, L. Wright, A. Mura, F. Levi, S. Robinson, A. Xuereb, B. Baptie, and D. Calonico, "Ultrastable laser interferometry for earthquake detection with terrestrial and submarine cables", *Science*, vol. 361, no. 6401, pp. 486–490, 2018. DOI: 10.1126/science.aat4458. eprint: https://www.science.org/doi/pdf/10.1126/science.aat4458. [Online]. Available: https://www.science.org/doi/abs/10.1126/science.aat4458.

[2] Z. Zhan, M. Cantono, V. Kamalov, A. Mecozzi, R. Müller, S. Yin, and J. C. Castellanos, "Optical polarization–based seismic and water wave sensing on transoceanic cables", *Science*, vol. 371, no. 6532, pp. 931–936, 2021. DOI: 10.1126/science.abe6648. eprint: https://www.science.org/doi/pdf/10.1126/science.abe6648. [Online]. Available: https://www.science.org/doi/abs/10.1126/science.abe6648.

[3] A. Mecozzi, M. Cantono, J. C. Castellanos, V. Kamalov, R. Muller, and Z. Zhan, "Polarization sensing using submarine optical cables", *Optica*, vol. 8, no. 6, pp. 788–795, Jun. 2021. DOI: 10.1364/OPTICA.424307. eprint: https://opg.optica.org/optica/abstract.cfm?URI=optica-8-6-788. [Online]. Available: https://opg.optica.org/optica/abstract.cfm?URI=optica-8-6-788.

[4] G. Marra, D. M. Fairweather, V. Kamalov, P. Gaynor, M. Cantono, S. Mulholland, B. Baptie, J. C. Castellanos, G. Vagenas, J.-O. Gaudron, J. Kronjäger, I. R. Hill, M. Schioppo, I. B. Edreira, K. A. Burrows, C. Clivati, D. Calonico, and A. Curtis, "Optical interferometry–based array of seafloor environmental sensors using a transoceanic submarine cable", *Science*, vol. 376, no. 6595, pp. 874–879, 2022. DOI: 10.1126/science.abo1939. eprint: https://www.science.org/doi/pdf/10.1126/science.abo1939. [Online]. Available: https://www.science.org/doi/abs/10.1126/science.abo1939.

[5] M. Mazur, J. C. Castellanos, R. Ryf, E. Börjeson, T. Chodkiewicz, V. Kamalov, S. Yin, N. K. Fontaine, H. Chen, L. Dallachiesa, S. Corteselli, P. Copping, J. Gripp, A. Mortelette, B. Kowalski, R. Dellinger, D. T. Neilson, and P. Larsson-Edefors, "Transoceanic phase and polarization fiber sensing using real-time coherent transceiver", in *Optical Fiber Communication Conference (OFC) 2022*, Optica Publishing Group, 2022, M2F.2. DOI: 10.1364/OFC.2022.M2F.2. eprint: https://opg.optica.org/abstract.cfm?URI=OFC-2022-M2F.2. [Online]. Available: https://opg.optica.org/abstract.cfm?URI=OFC-2022-M2F.2.

[6] M. Mazur, N. Parkin, R. Ryf, A. Iqbal, P. Wright, K. Farrow, N. K. Fontaine, E. Börjeson, K. Kim, L. Dallachiesa, H. Chen, P. Larsson-Edefors, A. Lord, and D. Neilson, "Continuous fiber sensing over field-deployed metro link using real-time coherent transceiver and das", in *European Conference on Optical Communication (ECOC) 2022*, Optica Publishing Group, 2022, Mo4A.2. [Online]. Available: https://opg.optica.org/abstract.cfm?URI=ECEOC-2022-Mo4A.2.

[7] M. Mazur, N. K. Fontaine, M. Kelleher, V. Kamalov, R. Ryf, L. Dallachiesa, H. Chen, D. T. Neilson, and F. Quinlan, "Continuous distributed phase and polarization monitoring of trans-atlantic submarine fiber optic cable", in *Optical Fiber Communication Conference (OFC) 2024*, Optica Publishing Group, 2024, Tu3J.1. DOI: 10.1364/OFC.2024.Tu3J.1. [Online]. Available: https://opg.optica.org/abstract.cfm?URI=OFC-2024-Tu3J.1.

[8] S. Guerrier, C. Dorize, E. Awwad, and J. Renaudier, "Introducing coherent MIMO sensing, a fading-resilient, polarization-independent approach to φ-OTDR", *Opt. Express*, vol. 28, no. 14, pp. 21 081–21 094, Jul. 2020. DOI: 10.1364/OE.396460. [Online]. Available: https://opg.optica.org/oe/abstract.cfm?URI=oe-28-14-21081.

[9] H. Awad, F. Usmani, S. Straullu, R. Bratovich, E. Virgillito, F. Aquilino, R. Proietti, and V. Curri, "Experimental validation for early earthquake detection using transfer learning", in *2025 Optical Fiber Communications Conference and Exhibition (OFC)*, 2025, pp. 1–3.

[10] H. Sun, M. Torbatian, M. Karimi, R. Maher, S. Thomson, M. Tehrani, Y. Gao, A. Kumpera, G. Soliman, A. Kakkar, M. Osman, Z. A. El-Sahn, C. Doggart, W. Hou, S. Sutarwala, Y. Wu, M. R. Chitgarha, V. Lal, H.-S. Tsai, S. Corzine, J. Zhang, J. Osenbach, S. Buggaveeti, Z. Morbi, M. I. Olmedo, I. Leung, X. Xu, P. Samra, V. Dominic, S. Sanders, M. Ziari, A. Napoli, B. Spinnler, K.-T. Wu, and P. Kandappan, "800G DSP ASIC Design Using Probabilistic Shaping and Digital Sub-Carrier Multiplexing", *Journal of Lightwave Technology*, vol. 38, no. 17, pp. 4744–4756, 2020. DOI: 10.1109/JLT.2020.2996188.

[11] S. J. Savory, "Digital coherent optical receivers: Algorithms and subsystems", *IEEE Journal of Selected Topics in Quantum Electronics*, vol. 16, no. 5, pp. 1164–1179, 2010. DOI: 10.1109/JSTQE.2010.2044751.

[12] A. Mecozzi, "Sensing with submarine optical cables", *APL Photonics*, vol. 9, no. 7, p. 070 902, Jul. 2024, ISSN: 2378-0967. DOI: 10.1063/5.0210825. eprint: https://pubs.aip.org/aip/app/article-pdf/doi/10.1063/5.0210825/20079137/070902_1_5.0210825.pdf. [Online]. Available: https://doi.org/10.1063/5.0210825.

[13] A. Mecozzi, C. Antonelli, M. Mazur, N. Fontaine, H. Chen, L. Dallachiesa, and R. Ryf, "Use of optical coherent detection for environmental sensing", *J. Lightwave Technol.*, vol. 41, no. 11, pp. 3350–3357, Jun. 2023. [Online]. Available: https://opg.optica.org/jlt/abstract.cfm?URI=jlt-41-11-3350.

[14] J. P. Gordon and H. Kogelnik, "PMD fundamentals: Polarization mode dispersion in optical fibers", *Proceedings of the National Academy of Sciences*, vol. 97, no. 9, pp. 4541–4550, 2000, ISSN: 0027-8424. DOI: 10.1073/pnas.97.9.4541. eprint: https://www.pnas.org/content/97/9/4541.full.pdf. [Online]. Available: https://www.pnas.org/content/97/9/4541.

[15] L. Rayleigh, "On waves propagated along the plane surface of an elastic solid", *Proceedings of the London Mathematical Society*, vol. s1-17, no. 1, pp. 4–11, 1885. DOI: https://doi.org/10.1112/plms/s1-17.1.4. eprint: https://londmathsoc.onlinelibrary.wiley.com/doi/pdf/10.1112/plms/s1-17.1.4. [Online]. Available: https://londmathsoc.onlinelibrary.wiley.com/doi/abs/10.1112/plms/s1-17.1.4.